PERGAMON

Organic Geochemistry 33 (2002) 655–663

Organic Geochemistry

www.elsevier.com/locate/orggeochem

Gas washing of oil along a regional transect, offshore Louisiana

Steven Losh*[,a], Lawrence Cathles[a], Peter Meulbroek[b]

[a]*Department of Geological Sciences, Cornell University, Ithaca, NY 14853, USA*
[b]*Department of Chemistry, California Institute of Technology, Pasadena, CA 91125, USA*

Abstract

Gas chromatogram data for 219 oils in a 190 km N–S transect offshore Louisiana reveal a spatially coherent pattern of compositional change which is caused by gas washing. Near the Louisiana shoreline, as much as 91% of the original *n*-alkanes have been removed from the oils. The maximum intensity of depletion decreases southward in a nearly regular fashion to nil at the Jolliet field 190 km offshore. The oils show a parallel change in the maximum carbon number of the removed *n*-alkanes, implying that the pressure at which gas washing took place also decreased in the offshore direction. The systematic change in maximum extent of depletion crosscuts tectonostratigraphic boundaries as well as oil source provinces. Models of gas washing suggest that the maximum depth of washing reflects the distribution of deeply buried continuous sands, suggesting deep sands may have provided sites for efficient gas–oil interaction. © 2002 Elsevier Science Ltd. All rights reserved.

1. Introduction

Migrating hydrocarbons in the subsurface are often multiphase. When a chemical mixture separates into two phases, the resultant phases can be quite distinct from the original mixture. For years, the partitioning of compounds between liquid and vapor phases in petroleum in the subsurface has been known, but the scale and intensity at which that process is known to operate has continually increased with time. Silverman (1965) demonstrated that gas exsolution from liquid oil during decompression modifies the composition of the oil. In most situations, however, compositional changes by this process are small, because they are limited by the amount of gas that can be dissolved in the oil and the amount of oil compounds that partition into that volume of vapor. Thompson (1987) broadened the scope of compositional change by introducing an 'evaporative fractionation' mechanism whereby variably-sized but possibly large batches of gas mix with oil and subsequently separate from it, removing *n*-alkanes preferentially to naphthenes and aromatics. Meulbroek (1997), Meulbroek et al. (1998) and Meulbroek (in press) expanded Thompson's concept by modeling a continuous gas stream that flows past and removes compounds from the oil in a process they referred to as 'gas washing'. Depending on the pressure and liquid composition, either evaporative fractionation or gas washing has the potential to remove nearly the entire mass of a liquid oil.

2. Calculation of *n*-alkane mass depletion

Thompson (1987) noted that separation of hydrocarbon vapor from a hydrocarbon liquid depletes the liquid in relatively high-fugacity compounds. Meulbroek (1997, in press) and Meulbroek et al. (1998) modeled the phase behavior of the *n*-alkanes. Low molecular weight *n*-alkanes are fractionated from liquid into a coexisting vapor phase preferentially to higher molecular weight *n*-alkanes. In this paper, we calculate the mass depletion of oil in *n*-alkanes, relative to an unfractionated oil, by gas washing in a 190 km long *N*-S transect offshore Louisiana. The calculation is simply a description of the mass depletion relative to an unaltered oil, and is independent of the actual cause of such depletion.

* Corresponding author.

0146-6380/02/$ - see front matter © 2002 Elsevier Science Ltd. All rights reserved.
PII: S0146-6380(02)00025-6

Mature unfractionated oils are typically characterized by exponential distribution of compounds, particularly *n*-alkanes, in homologous series (Kissin, 1987). Throughout the transect, as well as in an additional study area in which extensive equation of state modeling has been done (Meulbroek et al., 1998, in press), unfractionated oils display this exponential abundance distribution of *n*-alkanes. If abundance data for *n*-alkanes are converted to mole fractions and plotted as log(mole fraction of *n*-alkane of carbon number C_i) vs the carbon number, C_i, the plot (called a 'molar fraction plot') for an unfractionated oil is characterized by a straight line having the equation

$$\ln X_{n-C_i} = mC_i + b \quad (1)$$

(Kissin, 1987), where m is the slope of the plot, and b is the intercept. For unaltered oils, the slope of this best-fit line, termed the '*n*-alkane slope', is a function of oil maturity (3, 4, 5); the more mature the oil, the steeper (more negative) the slope. The *n*-alkane spectrum of a gas-washed oil comprises two parts: the unfractionated portion at high carbon numbers, where data are best fit by a straight line on the molar fraction plot, and a depleted portion at lower carbon numbers, which deviates from the straight line fit in a regular fashion. The *n*-alkane carbon number at which the two portions of the spectrum join is called the 'break number' by Meulbroek (1997). As shown by Thompson and confirmed by Meulbroek, the 'break number' is strongly affected by the pressure at which phase separation and attendant fractionation took place. The break number is much less affected by other variables in the gas washing process, including temperature and the amount of *n*-alkane that was fractionated, and is thus useful as a proxy for the pressure at which phase separation took place.

The slope of the unfractionated *n*-alkane spectrum beyond the break at $C_i > C_b$ (where C_b is the break number; Fig. 1) is used to re-create the unfractionated *n*-alkane spectrum, in conjunction with the requirement that all mole fractions of $n-C_i$ in the unfractionated oil add to unity. To avoid complications due to separator and sample handling losses, this analysis only incorporates *n*-alkanes having carbon numbers of 10 or higher. The *n*-alkane spectrum for the unfractionated oil has the same slope, but a different intercept than does the extrapolated best fit line through the data points. The intercept, b, for the unfractionated oil line is determined as follows.

As noted in Eq. (1),

$$\ln X_{nC_i} = mC_i + b,$$

where C_i = carbon number of compound i.

Exponentiating both sides, we have

$$X_{nC_i} = e^{mC_i+b} = e^{mC_i}e^{b} \quad (2)$$

We then impose the requirement that the sum of the mole fractions of compounds i is unity. We take the e^b term outside the summation, as it is a constant.

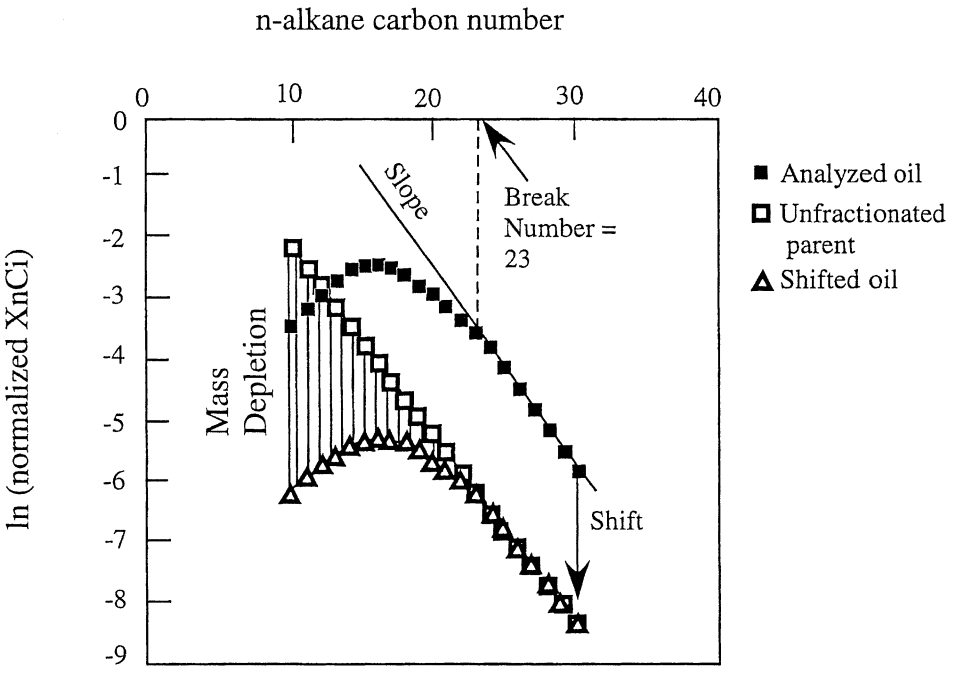

Fig. 1. Molar fraction plot, showing depleted and reconstructed *n*-alkane profile.

$$\Sigma X_{nC_i} = \Sigma e^{mC_i} e^b = e^b \Sigma e^{mC_i} = 1.0. \quad (3)$$

From the last equality, we rearrange to determine

$$e^b = 1/\Sigma e^{mC_i} \quad (4)$$

and finally, the intercept b is determined to be

$$b = -\ln \Sigma e^{mC_i} \quad (5)$$

Thus, the *n*-alkane spectrum for the unfractionated oil is defined in terms of Eq. (1), where the mole fractions sum to 1.0.

To determine the *n*-alkane mass depletion, the *n*-alkane spectrum of the analyzed oil is compared with the computed unfractionated spectrum, as shown in Fig. 1. For this analysis, the mole fractions of the analyzed sample must be normalized such they sum to 1.0. If both sets of points are plotted on the same molar fraction plot, it can be seen that the analyzed points are offset from the unfractionated oil points by a constant difference, f, for $C_i > C_b$.

$$f = \ln X_{nC_i} - (mC_i + b), \quad (6)$$

where X_{nC_i} pertains to *n*-alkane mole fractions in the analyzed oil, and $mC_i + b$ is the expression that describes the unfractionated oil. This equation is valid only for $C_i > C_b$.

The molar depletions of each compound can thus be computed directly as

$$\Delta \ln(\text{moles } nC_i) = mC_i + b - (\ln X_{nC_i} - f). \quad (7)$$

since X_{nC_i} = moles nC_i in the normalized *n*-alkane fraction. By subtracting f, and thereby shifting the *n*-alkane mole fractions in the analyzed oil to coincide with the calculated unfractionated oil *n*-alkane spectrum at $C_i > C_b$, the vapor is in effect being added back into the system. The shifted analyzed *n*-alkane data points represent the mole fractions of each *n*-alkane that is present within the liquid phase in the liquid + vapor mixture. The difference in molar fractions, hence moles, of each *n*-alkane between the fractionated sample and the calculated unfractionated parent is then readily expressed in terms of a depletion factor (DF) for each *n*-alkane. This factor is defined in terms of the fraction of each *n*-alkane that has been lost into the vapor phase:

$$DF = e^{\Delta \ln(\text{moles } nC_i)} \quad (8)$$

Introducing A as the number of moles of $n-C_i$ in the depleted oil, relative to the unfractionated oil, we have

$$A = e^{(mC_i + b)}/DF \quad (9)$$

Converting moles (X_{nC_i}) to mass (M_{nC_i}) by multiplying by the appropriate molecular weights, and defining Q as the *n*-alkane mass depletion fraction summed over all the *n*-alkanes heavier than $n-C_9$,

$$Q = 1 - \left(\Sigma M_{nC_i}\,(\text{analyzed oil}) / \Sigma M_{nC_i}\,(\text{unfract oil})\right) \quad (10)$$

The quantity Q defines the mass fraction of *n*-alkane that has been lost from an oil relative to its unfractionated parent.

One hundred sixteen oils were collected as part of a Gas Research Institute funded investigation of gas-related processes in the offshore Louisiana Gulf of Mexico Basin, and were analyzed by GCMS at Woods Hole Oceanographic Institution, under the direction of Jean Whelan. Additional data were contributed by Texaco (Tiger Shoals) and were also obtained from a previously established database for South Eugene Island Block 330 (Whelan et al., 1994). Whelan will report elsewhere on other aspects of oil composition. The quantification of gas–oil interaction constrains physical processes and geologic conditions under which gas interacted with oil, and we speculate on these constraints in the last part of this paper. The geologic controls on gas washing could have implications for exploration for deep hydrocarbons.

3. Transect data

3.1. Geologic and geochemical background

The transect along which the oils in this study were collected crosses distinct tectonostratigraphic provinces in the Gulf of Mexico (Fig. 2): the Oligocene-Miocene detachment province, the Miocene salt dome-minibasin province, the Plio-Pleistocene detachment province, and the tabular salt-minibasin province (Diegel et al., 1995). Mesozoic carbonate rocks and Cenozoic sand and mud comprise a 14-km thick section beneath the study area. Jurassic salt once underlay the thick sedimentary section, but has been largely remobilized into canopies and diapirs, once during the Eocene, and again during the late Miocene. Faulting and sedimentation in each of the four provinces reflects the interplay of deltaic and slope sedimentation with salt withdrawal at different times during the evolution of the sedimentary succession offshore Louisiana. Over time, near-coastal sands have prograded over more distal shales and slope/basin floor sands as deltas have built southward into the Gulf of Mexico, particularly during lowstands, leading to the present-day sedimentary package in which sands are generally thickest and most deeply buried near the present coastline.

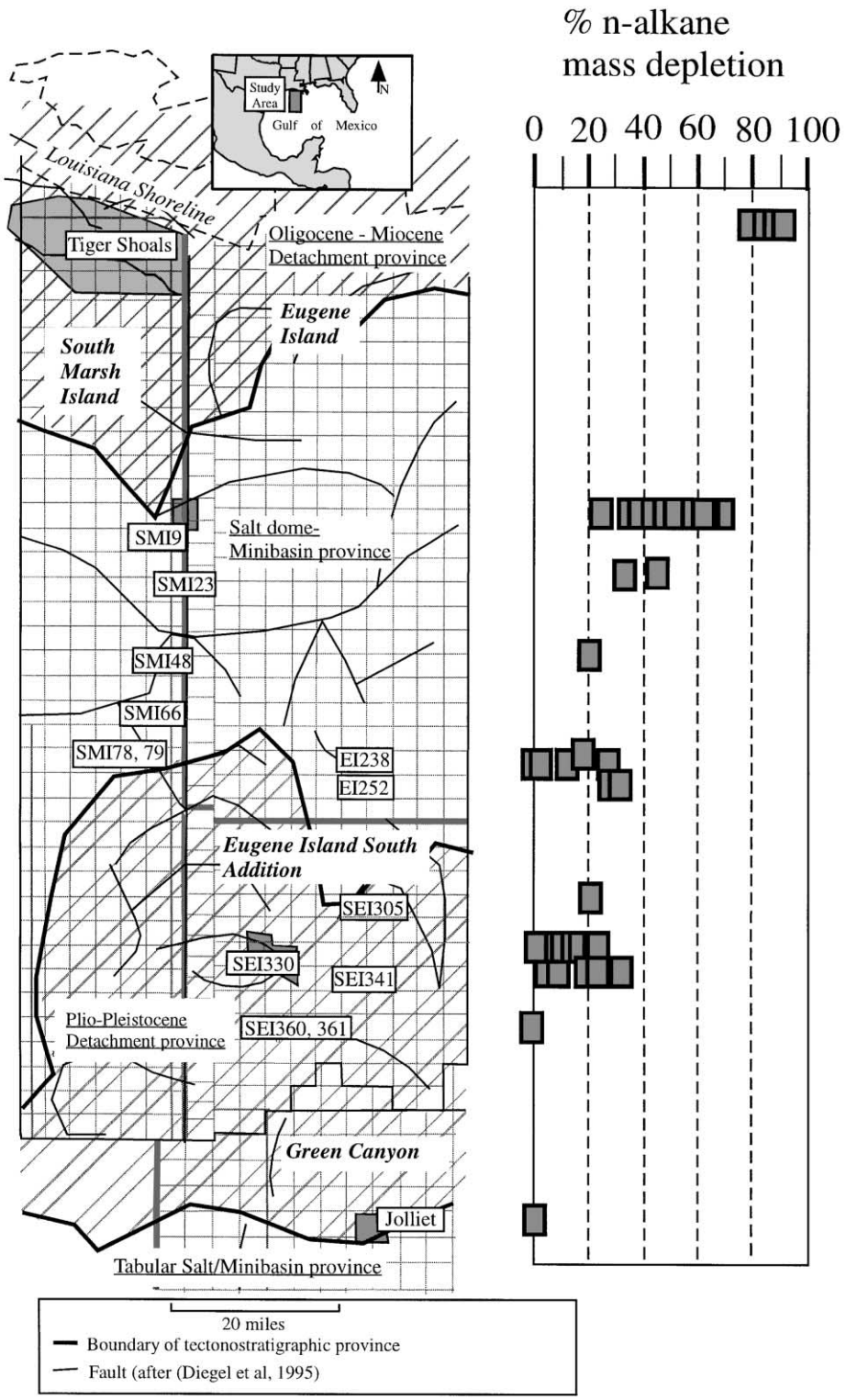

Fig. 2. Location map, showing sample sites, faults, and tectonostratigraphic provinces [after (6)]. Plot at right shows *n*-alkane mass depletion of oils from the transect, projected onto a north-south line at the same scale as the map. Maximum *n*-alkane depletion shows a pronounced decrease from north to south.

Oil samples were collected mainly from 4 sites, with additional samples collected between sites. In each site we have compiled the geology, present fluid pressure, porosity data (as indicators of past fluid pressures), and oil and gas chemistry. The Tiger Shoals study area, nearest the shoreline, covers about 500 km^2 and comprises six fields in faulted Miocene sands, containing total initial reserves of 176 MMbbl liquids (130 MMbbl oil and 46 MMbbl condensate) and 6.4 Tcf gas. The SMI9 field contains 14 MMbbo and 135 bcf gas in Miocene sands adjacent to a salt diapir. The SEI330 field, described in detail by Holland et al. (1990) and Alexander and Flemings (1995), contains 307 MMbbo and 1.5 Tcf gas in Plio-Pleistocene sands within a salt-withdrawal minibasin. The Jolliet field contains 32 MMbbo and 152 Bcf gas in faulted middle to late Pleistocene levee and channel sands in a slope fan/basin floor fan complex atop a salt sheet (Cook and D'Onfro, 1991). These fields sample a range of sediment ages and geologic settings in the Gulf of Mexico, and contain oil of varying maturity and from different sources.

Oils along the transect are sourced predominantly from Tertiary and possibly Cretaceous shale nearshore (eg. Tiger Shoals and SMI9 fields) and predominantly from Jurassic marls on the outer shelf and slope (eg. SEI330 and Jolliet fields) (Thompson et al., 1990; Hood et al., 1995). Samples from the Tiger Shoals area, near the Louisiana coastline, have equivalent vitrinite reflectance (calculated from MPI1, Radke, 1988) between 1.0 and 1.2% Ro, consistent with relatively steep *n*-alkane

Table 1
Average depths, break numbers, and *n*-alkane mass depletion fractions for transect oils

Field	Sand	Depth	Break no.	*n*-alkane depl
Tiger	M	8585	23	0.82 (1)[a]
Shoals	Tex L	9450	22–23	0.82 (2)
	N	9661	23	0.86 +/− 0.02 (8)
	T2A	10820	23	0.87 (1)
	U	11340	23	0.88 +/− 0.03 (5)
	V	11210	23	0.91 (2)
	12000	12200	24	0.83 (1)
	Rob L	14250	23–24	0.88 (4)
SMI9	10200	10179	16	0.39 (1)
	11300	10789	18	0.51 (2)
	11900	12200	17–19	0.46 +/− 0.06 (8)
	12200	12172	17–21	0.52 +/− 0.08 (6)
	15700	15000	15–20	0.47 +/− 0.12 (7)
	17800	16500	16–17	0.25 (2)
SMI23		12373–14175	18	0.36–0.47 (2)
SMI48		10256	18	0.22 (1)
SMI79		12144–14156	15	0.18 (1)
EI238, 252		7760–13450	12–16	0–0.30 (7)
SEI305		8950–12050	12–16	0.21 (3)
SEI330	GA	4200	–	–
	HB	4800	–	–
	JD	6242		[b]
	LF	6792	0[c],14–15	0.10 (2)
	MG	7018	0	
	NH	7332		0
	OI	7156	11–16	0.08 +/− 0.03 (14)
SEI341		5650–7381	13–16	0.05–0.33 (6)
SEI360, 361		3300–4595	0	0 (2)
Jolliet	GS/GJ	6008		0 (3)
	HJ	6825		0 (4)
	HO/IA	7123		0 (4)
	IF	7388		0 (3)
	KE	8900		0 (1)
	KP/KQ	8562		0 (1)
	KS	10090		0 (1)

[a] Number of samples is in parentheses.
[b] Samples are condensate, which are not evaluated for break number or mass depletion.
[c] Break number of zero indicates that oil is unfractionated.

slopes of -0.30 ± 0.03 (see Kissin, 1987; Meulbroek, 1997). Oils at SEI330 are shown by Whelan et al. (1994) to have equivalent vitrinite reflectance maturity of $0.80\pm0.05\%$ Ro. Most samples from the other fields comprising the transect have maturity similar to or slightly higher than the SEI330 oils (J. Whelan, unpub data). Thus, the transect sampled oils from different sources and of a range of maturities from middle to late oil window, as well as from different tectonostratigraphic provinces.

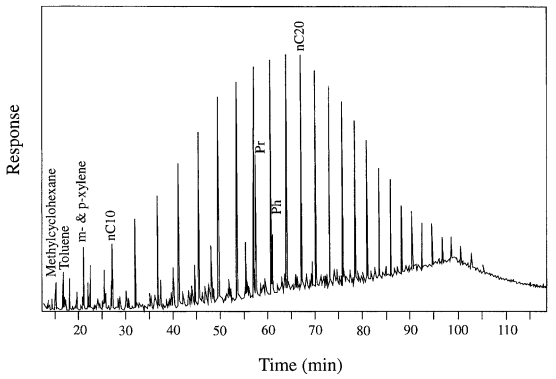

Fig. 3. Gas chromatogram of a gas-washed oil, with selected peaks labeled. Note profound depletion of naphthenes and aromatics as well as light *n*-alkanes, and dominance of heavier *n*-alkanes. Sample is from the SMI9 field.

3.2. n-*alkane depletion of transect oils*

The *n*-alkanes of transect oils have been depleted in a systematic manner, both in a given oil and over the length of the transect (Fig. 2, Table 1). Fig. 3 shows a representative gas chromatogram of an oil from SMI9, whereas Fig. 4a–d shows representative molar fraction plots for oils from north (Tiger Shoals) to south (Jolliet). As noted earlier, unfractionated oil plots as a straight line on this kind of plot.

Fractional *n*-alkane mass depletion and maximum break number from a sampled field both decrease with distance from the shoreline (Table 1, Figs. 2 and 5). *n*-Alkane mass depletions of 76–91%, and break numbers of 22–24, characterize oils from the Tiger Shoals study area, near the Louisiana shoreline. SMI9 oils have lower *n*-alkane mass depletions (20–62%) and break numbers (16–20). SEI330 oils show variable depletion: many show linear trends (no depletion) on the molar

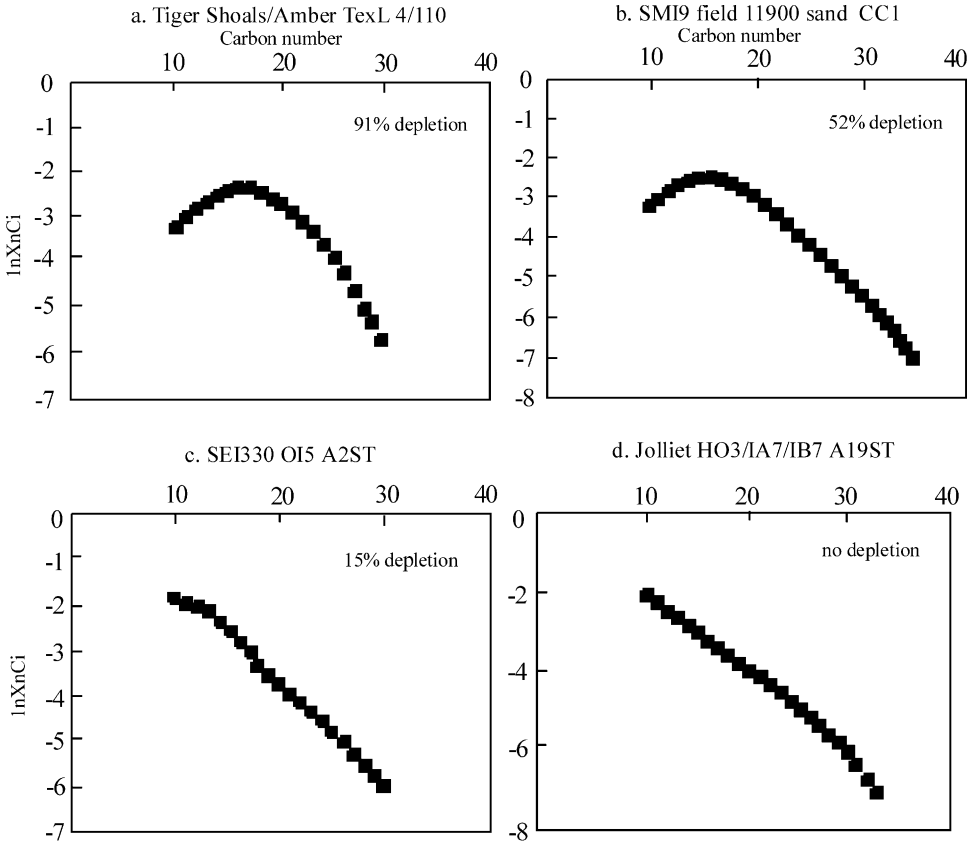

Fig. 4. Molar fraction plots of oils from north (a) to south (d).

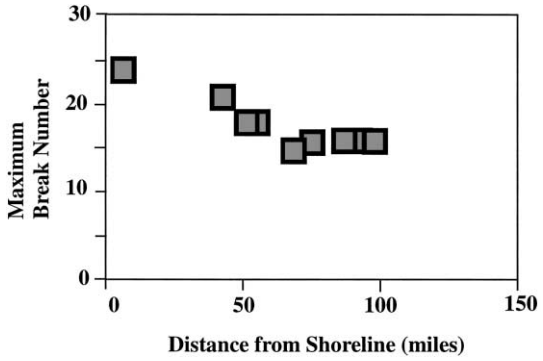

Fig. 5. Maximum oil break number, at a sampled field, vs distance from shoreline.

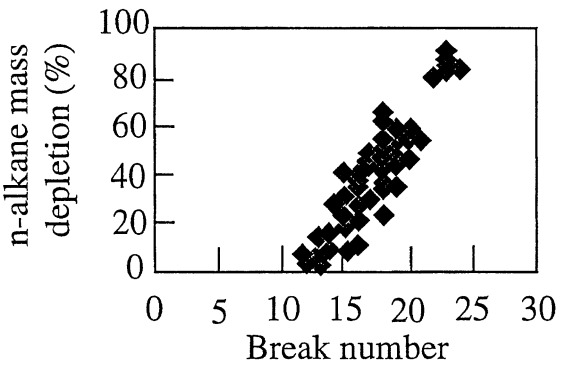

Fig. 6. Oil break number vs *n*-alkane mass depletion.

fraction plot, and the maximum depletion (15%) and break number (16) are significantly lower than in samples closer to the shoreline. Finally, oils from Jolliet show no depletion. This trend, corroborated by samples collected from other locations between the four main GRI study sites, overprints variations in both geology and oil source and maturity.

4. Discussion

Gas washing of oil can be distinguished from other processes that alter an oil's *n*-alkane distribution, notably biodegradation and water washing. The *n*-alkane pattern is not a result of biodegradation for the following reasons. (1) The oils used for analysis of gas washing in this paper are unbiodegraded as determined by their having pristane/heptadecane ratios less than one (e.g. Curiale and Bromley, 1996); the great majority are less than 0.8. Many of these oils have had *n*-alkanes as heavy as triacontane (at Tiger Shoals) and eicosane (at SMI9) removed. If biodegradation were responsible for this, the Pr/nC17 ratio would be accordingly high. As it is, the process that removed the *n*-alkanes also removed iso-alkanes, a pattern consistent with gas washing. (2) A characteristic of gas washing is the essentially exponential distribution of *n*-alkane mass depletions at carbon numbers less than the break number, and the removal of low-molecular weight aromatics and naphthenes as well as *n*-alkanes. Biodegradation affects *n*-alkanes in the same carbon number range as gas washing, but the depletions tend to be either uneven, and the *n*-alkane spectrum 'ratty', or biodegradation eradicates the entire *n*-alkane spectrum. In either case, the significant biodegradation that is needed to produce large *n*-alkane depletions also typically results in an unresolved complex hump that is absent in even heavily gas-washed oils. (3) The presence of mid-range *n*-alkanes (i.e. *n*C15) in an oil that has lost nearly all of its light aromatics and naphthenes (Fig. 3) is not characteristic of a biodegraded oil (e.g. Peters and Moldowan, 1993). Such an oil is also compositionally distinct from commonly-observed oils that have been biodegraded and then mixed with a young, unbiodegraded condensate. Such oils show light-end enrichments and unresolved complex that are both absent from gas-washed oils, and are also readily identifiable on the molar fraction plot by a steep *n*-alkane slope at low carbon numbers coupled with a less steep slope at higher carbon numbers.

Water washing shares with gas washing the capacity to fractionate low molecular weight compounds from the oil relative to heavier ones, but differs in the relative solubilities of compounds, decreasing in the order aromatics, *n*-alkanes, naphthenes (Lafargue and Barker, 1988). These workers found that even relatively minor water washing strongly depletes an oil in toluene and naphthalenes compared to a relatively insoluble *n*-alkane such as *n*C20. A number of oils that display substantial *n*-alkane depletion nonetheless contain significant toluene (2–5 g/l). The presence of significant concentrations of other aromatics (naphthalenes, phenanthrene, dibenzothiophene) in oils that have undergone strong *n*-alkane depletion also points to gas washing rather than water washing as the primary, if not sole, cause of that depletion (cf. Palmer, 1984).

Other processes that affect oil composition can also be ruled out as causes for the observed oil compositional patterns. Paraffin precipitation affects *n*-alkanes at the high carbon-number end of the molar fraction plot, and is thus not readily confused with the effects of gas washing which, at least in this study, only affects compounds as heavy as triacontane. Gas cap separation, fractionation in the separator, and short-term evaporation of sample after collection are shown by Meulbroek (1997) and Meulbroek et al. (1998) to affect compounds only as heavy as decane or so, depending on actual reservoir or separator pressures. As noted earlier, to avoid any complications from production-related compositional effects, the *n*-alkane depletion computations in this paper do not incorporate *n*-alkanes having car-

bon numbers less than 10. In addition, gas washing also involves large ratios of gas to oil. Meulbroek et al. (1998) concluded that oils at the SEI330 field interacted with up to 14 mol of gas/mol of oil, or about 18 volumes of gas per volume of oil at reservoir conditions. This volume of gas far exceeds that which can dissolve in oil at any one time, and requires the mixing of oil with, and separation from, a migrating gas stream, ruling out gas cap separation or migration fractionation at reservoir conditions as an explanation for the observed *n*-alkane distributions. For these reasons we believe that the extensive, systematic depletion of oils in *n*-alkanes heavier than decane must be attributed to their removal in a vapor phase.

The break number covaries linearly with fractional *n*-alkane mass depletion as shown in Fig. 6. This correlation is not necessarily required: gas washing at relatively low pressure can nonetheless involve a large gas:oil volume, and an oil with a low break number can thus display a relatively large *n*-alkane depletion. Since the 'break number' depends primarily on the pressure at which gas washing occurred, the correlation of break number and mass depletion indicates that a greater fraction of oil was removed by washing at greater depths. This is partly due to the higher solubility of all *n*-alkanes in hydrocarbon gas at higher pressure, but also reflects the interaction of a greater mass of methane with each gram of oil in the north compared to the south.

Geologic factors that control the occurrence of gas washing can be evaluated by reconstructing the framework in which gas washing took place at specific locations. Equation of state (EOS) modeling (Meulbroek, 1997) of oil–gas interactions at South Eugene Island Block 330 indicates that gas washing of oils there took place at pressures on the order of 6000 psi for fractionated oils with break numbers of 16. Even for these modestly-depleted oils (15% maximum), the volume of gas per volume of oil is large—on the order of 18:1 at reservoir conditions (Meulbroek et al., 1998). Given the present-day fluid pressure profile, and extrapolations to past profiles at the time of oil migration (i.e. Gordon and Flemings, 1998), this gas washing took place at depths of 2.5–2.9 km. Sediments that lay at that depth at 300 kA, which is the maximum age of reservoir filling (Losh, 1998), are now buried to depths of 3.0–3.4 km. This corresponds to the present depth of the *Lenticulina* 1 sand, a slope fan which comprises a deep, continuous sand within the minibasin (Alexander and Flemings, 1995). It contains gas and underlies the oil-bearing reservoir section. A similar relationship between gas washing depth and lithostratigraphy exists in the Tiger Shoals study area. Based on EOS/phase equilibria modeling, the oils at Tiger Shoals were gas washed relatively recently at pressures on the order of 10,000 psi. Such pressures correspond with one of the deepest continuous sands in the Tiger Shoals area, the Robulus L. This sand produces oil in one of the fields in the area, the Starfak. Thus, EOS modeling results, combined with information regarding fluid pressure evolution, migration timing, and burial history, suggests gas washing may occur in deep, continuous sand not far below or at the base of the reservoir section in a particular field.

The regularity of the spatial trends in maximum break number and *n*-alkane mass depletions, despite variations in oil source and maturity as well as tectonostratigraphic province, indicates that the factors that exert a first-order control on gas washing overrides the effects of initial oil composition. The decrease in pressure, hence (to a first approximation) depth, of gas washing with distance from the shoreline implies that one of the main controls also varies regularly with distance from the shoreline, in such a way that gas washing takes place at shallower depths farther offshore. Perhaps the most salient feature that varies in such a manner is the maximum depth of continuous sands. As previously noted, sand is generally found to much greater depths near shore than on the continental slope. The linkage of the greatest depth of gas washing in an area with a deep, continuous sand in two of our study areas implies that deep sands may provide suitable locations for washing of oil with gas generated later or from a different source. The depth to the first significant sand encountered by ascending hydrocarbons, the local fluid pressure profile, and the thermal history of the oil and gas source rocks, may be the most important factors controlling the depth and local intensity of gas washing.

The lack of gas washed oil at Jolliet, where sands are known to depths of 3 km and gas is currently venting, is clearly not due to a lack of sand at appropriate depths nor to a lack of a vapor phase, but may rather reflect the effect of short-range sand heterogeneity on gas washing. At Jolliet, oil and gas may have migrated along pathways that are far enough apart that they each intersect different channels, which are spatially restricted (e.g. Rowan, 1995). Also, basin modeling shows that considerably less sediment has entered the gas generation window in the deep water areas off the continental slope than near shore. The presence of light oil/condensate overprinting older, biodegraded oil at Jolliet may be indicative of a vapor phase associated with gas washing of oil beneath the existing field.

5. Conclusion

Gas washing of oil along a transect in the Gulf of Mexico varies from profound nearshore to nil in a continental slope setting 190 km offshore. This variation in maximum extent of gas washing with distance from shore is remarkably regular, despite variations in tectonostratigraphic setting and oil source and maturity. It

correlates, roughly at least, with the depth to the deepest known extensive sand in two of our study areas. We suggest that gas washing may take place in or near the first continuous sand encountered by oil and gas along their respective migration pathways. Through equation of state modeling and placing samples in their proper geologic and geochemical context, analysis of the extent and nature of gas washing could indicate the existence of a continuous 'mixing' sand which might itself be an exploration target.

Acknowledgements

This work has been funded by the Gas Research Institute, as part of its project, 'Seal Control on Hydrocarbon Migration: Physical and Chemical Consequences' (Contract no. 5097–260–3787 to Larry Cathles, with subcontract to Jean Whelan, Woods Hole Oceanographic Institution). GC analyses for oil samples collected for this study were carried out in the laboratory of Dr. Jean Whelan, Woods Hole Oceanographic Institution. We thank Texaco EPTD for use of their data from Tiger Shoals.

References

Alexander, L., Flemings, P., 1995. Geologic evolution of a Pliocene-Pleistocene salt withdrawal mini-basin, Eugene Island, Block 330, offshore Louisiana. Am. Assoc. Petrol Geol. Bull 79, 1737–1756.

Cook, D., D'Onfro, P., 1991. Joliet Field thrust structure and stratigraphy, Green Canyon Block 184, offshore Louisiana. Trans. Gulf Coast Assoc. Geol. Socs. 41, 100–121.

Curiale, J., Bromley, B., 1996. Migration induced compositional changes in oils and condensates of a single field. Org. Geochem. 24, 1097–1113.

Diegel, F., Karlo, J., Schuster, D., Shoup, R., Tauvers, P., 1995. Cenozoic structural evolution and tectonostratigraphic framework of the northern Gulf Coast continental margin In: Jackson, M.P.A., Roberts, D., Snelson, S. (Eds.), Salt Tectonics: A Global Perspective. Am. Assoc. Petrol. Geol. Tulsa OK, 1995, pp. 109–151, Memoir 65.

Gordon, D., Flemings, P., 1998. Generation of overpressure and compaction-driven fluid flow in a Plio-Pleistocene growth faulted basin, Eugene Island 330 field, offshore Louisiana. Water Resour. Res. 10, 177–196.

Holland, D., Leedy, J., Lammlein, D., 1990. Eugene Island Block 330 field—USA offshore Louisiana. In: Beaumont, E., Foster, N. (Eds.), Treatise in Petroleum Geology: Structural Traps III: Tectonic Fold and Fault Traps. Am. Assoc. Petrol. Geol., Tulsa, OK, pp. 103–143.

Hood, K., Wenger, L., Gross, O., Harrison, S., Goodoff, L., 1995. Northern Gulf of Mexico; an integrated approach to source, maturation, and migration. Am. Assoc. Petrol. Geol. Abstr. w/Prog 4, 109–110.

Kissin, Y., 1987. Catagenesis and composition of petroleum: origin of *n*-alkanes and isoalkanes in petroleum crudes. Geochim. et Cosmochim. Acta 51, 2445–2457.

Lafargue, E., Barker, C., 1988. Effect of water washing on crude oil compositions. Am. Asoc. Petrol. Geol. Bull. 72, 263–276.

Losh, S., 1998. Oil migration in a major growth fault: structural analysis of the Pathfinder core, South Eugene Island Block 330, offshore Louisiana. Am. Assoc. Petrol. Geol. Bull. 82, 1694–1710.

Meulbroek, P., 1997. Hydrocarbon phase fractionation in sedimentary basins. PhD thesis, Cornell University, Ithaca, NY.

Meulbroek, P., Cathles, L., Whelan, J., 1998. Phase fractionation at South Eugene Island Block 330. Org. Geochem 29, 223–239.

Meulbroek, P., 2002. Equations of state in exploration. Org. Geochem. 33, this issue.

Palmer, S., 1984. Effect of water washing on C15+ hydrocarbon fraction of crude oils from northwest Palawan, Philippines. Am. Assoc. Petrol. Geol. Bull. 68, 137–149.

Peters, K., Moldowan, M., 1993. Biomarker Guide. Prentice-Hill, Englewood Cliffs, NJ.

Radke, M., 1988. Application of aromatic compounds as maturity indicators in source rocks and crude oils. Marine and Petrol. Geol. 5, 224–235.

Rowan, M., 1995. Structural styles and evolution of allocthonous salt, central Louisiana outer shelf and upper slope. In: Jackson, M.P.A., Roberts, D., Snelson, S. (Eds.), Salt Tectonics: A Global Perspective. Am. Assoc. Petrol. Geol. Tulsa, OK, pp. 209–228, Memoir 65.

Silverman, S., 1965. Migration and segregation of oil and gas. In: Young, A., Galley, G. (Eds.), Fluids in Subsurface Environments, vol. 4. Am. Assoc. Petrol. Geol. Mem., pp. 53–65.

Thompson, K., 1987. Gas condensate migration and oil fractionation in deltaic systems. Marine Petrol. Geol. 5, 237–246.

Thompson, K., Kennicutt, M., Brooks, J., 1990. Classification of offshore Gulf of Mexico oils and gas condensates. Am. Assoc. Petrol. Geol. Bull. 74, 188–198.

Whelan, J., Kennicut, M., Brooks, J., Schumacher, D., Eglinton, L., 1994. Organic geochemical indicators of dynamic fluid flow processes in petroleum basins. Org. Geochem. 22, 587–615.